

Nonlinear Post-Buckling Analysis of Isotropic Plates Using Finite Strip Methods

S.A.M. Ghannadpour¹, H.R. Ovesy² and M. Nassirnia³

This paper presents the theoretical developments of two finite strip methods, i.e. semi-analytical and full-analytical, for the post-buckling analysis of isotropic plates. In the semi-analytical finite strip approach, all the displacements are postulated by the appropriate shape functions while in the development process of the full-analytical approach, the Von-Karman's equilibrium equation is solved exactly to obtain the buckling loads and the out-of-plane buckling deflection modes. The investigation of the plates' buckling behaviour is then extended to the post-buckling study with the assumption that the deflected form after the buckling is a combination of the first, second and higher (if required) modes of buckling. Thus, the full-analytical post-buckling study is an effective multi term analysis. In this method, the Von-Karman's compatibility equation is used together with a consideration of the total strain energy of the strut. Through the solution of the compatibility equation, the in-plane displacement functions, which are themselves related to the Airy stress function, are developed in terms of the unknown coefficients in the assumed out-of-plane deflection function. The in-plane and out-of-plane deflection functions are substituted in the total strain energy expressions and the theorem of minimum total potential energy is applied to solve for the unknown coefficients.

INTRODUCTION

Prismatic plates and plate structures are increasingly used as structural components in various branches of engineering, particularly in aerospace and marine engineering. These structures are often employed in situations where they are subjected to in-plane compressive loading. In aerospace engineering, in particular, the quest for efficient, light-weight structures often leads to allowing for the possibility of local buckling and post-local-buckling at design load levels. Thus, it is

important to accurately predict the buckling and post-buckling behavior of such structures.

There are a lot of papers concerning linear buckling and vibration analysis of composite laminated plates and plate structures formed of composite materials having very general material properties [1-5]. They have extensively used the Finite Strip Method (FSM) based on the use of Classical Plate Theory (CPT), first-order Shear Deformation Plate Theory (SDPT) and Higher-order Shear Deformation Plate Theory (HSDPT). The post-local-buckling behavior of elastic plates or plate structures is a geometric non-linear problem. The non-linearity occurs as a result of relatively large out-of-plane deflections, which necessitates the inclusion of non-linear terms in the strain-displacement equations. The early works concerned with the use of the FSM in predicting the geometrically non-linear response of single rectangular plate and prismatic plate structures are those of Graves Smith and Sridharan [6], [7] and Hancock [8]. These authors consider the post-buckling behavior of plates with simply supported ends when subjected to

-
1. *Corresponding Author, Assistant Professor, Dept. of Aerospace Eng., Faculty of New Technologies and Engineering, Shahid Beheshti University, G.C., Tehran, Iran, Email: A_ghannadpour@sbu.ac.ir.*
 2. *Professor, Dept. of Aerospace Eng., Center of Excellence in Computational Aerospace Eng., Amirkabir Univ. of Tech., Tehran, Iran.*
 3. *M.Sc. Student, Dept. of Aerospace Eng., Center of Excellence in Computational Aerospace Eng., Amirkabir Univ. of Tech., Tehran, Iran.*

progressive end shortening. They also consider the post-buckling behavior of plate structures subjected to uniform or linearly varying end shortening with each component plate of the structure having simply supported ends. The elastic post-buckling response of channel section struts and rectangular box columns have been investigated by Graves Smith and Sridharan. Hancock has used the finite strip method to investigate the post-buckling behavior of square box and I-section columns. In the finite strip methods developed by the aforementioned authors, in-plane displacement fields are postulated in addition to the out-of-plane displacement field. The lengthwise variations in the displacement fields are trigonometric functions. The crosswise variations in both in-plane and out-of-plane displacement fields are simple polynomial functions. It is noted that the above-mentioned finite strip methods can be categorized as Semi-analytical FSM (S-a FSM). Ref. [9] provides a fairly state-of-the-art summary on the use of the semi-analytical finite strip method (S-a FSM) as well as the spline finite strip method. It is worth mentioning that there are two papers, written by Rhodes [10] and Chou & Rhodes [11], which are extremely useful in providing references on the theoretical (mostly based on the semi-energy method) and experimental research into thin-walled structures.

Khong and Rhodes [12] have set up a computationally efficient approach to the post-buckling analysis of prismatic structural members. In this approach, a linear finite strip method, developed for the buckling analysis, based on the Principle of Minimum Potential Energy is employed to find the buckling eigenvector. This eigenvector is then used as the post-buckled deflected shape in a single-term post-buckling analysis based on the Principle of Minimum Potential Energy. The analysis is simplified by the assumption that stresses in the direction perpendicular to loading and shear stresses have negligible effects. This approach can be considered as a lower bound method of post-buckling analysis (*i.e.* the post-buckling stiffness of the structure is underestimated by this approach). The method is applied to plain and stiffened channel sections as well as Z-sections.

Ovesy *et.al.* [13-15] have developed a Semi-energy post-local-buckling FSM in which the out-of-plane displacement of the finite strip is the only displacement which is postulated by a deflected form. The developed Semi-energy FSM (S-e FSM) has been applied to analyze the post-local-buckling behavior of thin flat plates [13], open channel section [14] and box section struts [15]. More recently, Ghannadpour and Ovesy [16-20] have developed a full-analytical post-local-buckling FSM in which the solution of the Von-Karman's equilibrium equation was substituted into the Von-Karman's compatibility equation. It is noted that in their analysis, only one of the calculated out-of-

plane buckling deflection modes, corresponding to the lowest buckling load, *i.e.* the first mode, is used for the initial post-buckling study. For this reason, their method was designated by the name single-term Full-analytical Finite Strip Method (F-a FSM). It is worth mentioning that the single-term assumption within F-a FSM analysis corresponds to the fact that the shape of the plate in the post-buckling region is unchangeable in both longitudinal and transverse directions. Thus, the relationship between load and end-shortening becomes a linear function.

In the current paper, the theoretical developments of a high accuracy multi-term F-a FSM for the post-buckling analyses of some isotropic plates are attempted. The strip is developed based on the concept that it is an effective plate, and thus the Von-Karman's equilibrium equation is solved exactly to obtain the buckling loads and the corresponding forms of out-of-plane buckling deflection modes. In order to solve the Von-Karman's compatibility equation, the deflected form after the buckling is assumed as a combination of the first, second and higher (if required) modes of buckling. Subsequently, the general form of in-plane displacement fields in post-buckling region can be obtained. This method is characterized by the use of buckling mode shapes, obtained from the Von-Karman's equilibrium equation, as global shape functions for representing displacements in a geometrically non-linear analysis. The in-plane and out-of-plane deflection functions are substituted in the total strain energy expressions and the theorem of minimum total potential energy is applied to solve for the unknown coefficients.

THEORETICAL DEVELOPMENTS OF THE FULL-ANALYTICAL FSM

The detailed fundamental elements of the theory have been given in earlier publications by Ghannadpour and Ovesy [16-20]. It is noted that a perfectly flat high accuracy strip made up of a linear isotropic material (with a constant modulus of elasticity E and Poisson ratio ν) is assumed throughout the paper. The so-called high accuracy finite strip is assumed to be simply supported out-of-plane at the loaded ends, and to be thin so that the Classical Plate Theory (CPT) is applied in the remainder of the paper. The finite strip, which is schematically shown in Figure 1, is of the length L , width b and thickness t .

The Von-Karman's equilibrium and compatibility equations for large deflections of plate with the assumption that the normal pressure is zero are given by the following equations, respectively.

$$D\nabla^4 w - t (F_{,yy} w_{,xx} - 2F_{,xy} w_{,xy} + F_{,xx} w_{,yy}) = 0 \quad (1a)$$

$$\nabla^4 F = E (w_{,xy}^2 - w_{,xx} w_{,yy}) \quad (1b)$$

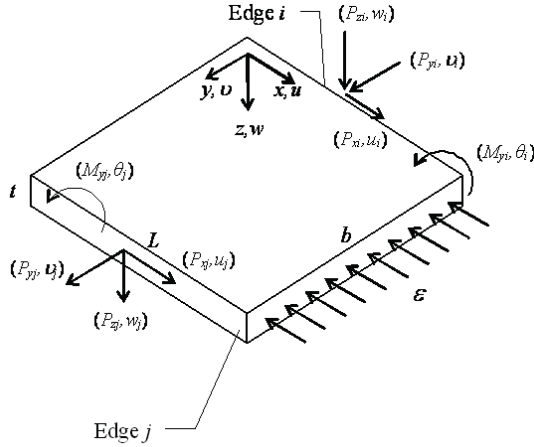


Figure 1. A typical high accuracy finite strip.

In this equation, the function F is known as the Airy stress function. The positive directions of the edge forces/moments and displacements are shown in Figure 1. It can be seen in Figure 1 that the nodal line forces and moments can be expressed in terms of internal in-plane forces and normal displacements on the edges as follows:

$$\begin{cases} P_{xi} = -N_{xy} |_{y=0} \\ P_{xj} = N_{xy} |_{y=b} \\ P_{yi} = -N_y |_{y=0} \\ P_{yj} = N_y |_{y=b} \\ P_{zi} = D[w_{,yyy} + (2-\nu)w_{,xxy}]_{y=0} \\ P_{zj} = -D[w_{,yyy} + (2-\nu)w_{,xxy}]_{y=b} \\ M_{yi} = -D[w_{,yy} + \nu w_{,xx}]_{y=0} \\ M_{yj} = D[w_{,yy} + \nu w_{,xx}]_{y=b} \end{cases} \quad (2)$$

In the above equation, N_y and N_{xy} are the membrane direct and shearing stress resultants per unit length. It is noted that in the remainder of the paper, the subscripts $0,1,2$ are used for pre-buckling, buckling and post-buckling stages, respectively.

Buckling analysis

The out-of-plane buckling deflection mode w_1 is obtained by trying to solve the Von-Karman's equilibrium equation, *i.e.* Eq. (1-a). This gives:

$$D\nabla^4 w_1 - t(F_{0,yy} w_{1,xx} - 2F_{0,xy} w_{1,xy} + F_{0,xx} w_{1,yy}) = 0 \quad (3)$$

where $\nabla^4 w_1 = w_{1,xxxx} + 2w_{1,xxyy} + w_{1,yyyy}$. In the pre-buckling stage, the strip is subjected to the compressive axial stress σ and thus:

$$D(w_{1,xxxx} + 2w_{1,xxyy} + w_{1,yyyy}) + t\sigma w_{1,xx} = 0 \quad (4)$$

A separable form is assumed for the displacement w_1 in order to reduce the above partial differential equation into an ordinary differential equation. The out-of-plane buckling deflection mode w_1 is assumed to vary sinusoidally with x . This assumption is consistent with the simply supported boundary conditions at the loaded ends. Thus:

$$w_1(x, y) = f_{w1}(y) \cdot \sin(\lambda x) \quad (5)$$

where $\lambda = \bar{n}\pi/L$ and parameter \bar{n} in the above displacement function is merely an integer which represents the number of buckle half-wavelengths along the strip, and $f_{w1}(y)$ represents the shape function in the transverse direction y . Substituting out-of-plane buckling deflection mode w_1 from Eq. (5) into Eq. (4) and rearranging it leads to the following fourth-order ordinary differential equation:

$$f_{w1}'''' - 2\lambda^2 f_{w1}'' + \lambda^4(1-\zeta)f_{w1} = 0 \quad (6)$$

where $\zeta = \sigma t/\lambda^2 D$ and the superscript ' denotes differentiation with respect to y , *i.e.* $(\)'$. The solution of Eq. (6) depends on whether ζ , which is clearly positive, is greater than, less than, or equal to unity.

For $\zeta > 1$, the solution can be written as:

$$\begin{aligned} f_{w1}(y) = & C_{w1}^{(1)} \cosh(\alpha \lambda y) + C_{w1}^{(2)} \sinh(\alpha \lambda y) \\ & + C_{w1}^{(3)} \cos(\beta \lambda y) + C_{w1}^{(4)} \sin(\beta \lambda y) \\ \alpha = & \sqrt{1 + \sqrt{\zeta}} \quad \beta = \sqrt{-1 + \sqrt{\zeta}} \end{aligned} \quad (7)$$

while for $0 < \zeta < 1$,

$$\begin{aligned} f_{w1}(y) = & C_{w1}^{(1)} \cosh(\alpha \lambda y) + C_{w1}^{(2)} \sinh(\alpha \lambda y) \\ & + C_{w1}^{(3)} \cosh(\beta \lambda y) + C_{w1}^{(4)} \sinh(\beta \lambda y) \\ \alpha = & \sqrt{1 + \sqrt{\zeta}} \quad \beta = \sqrt{1 - \sqrt{\zeta}} \end{aligned} \quad (8)$$

and for $\zeta = 1$,

$$\begin{aligned} f_{w1}(y) = & C_{w1}^{(1)} \cosh(\sqrt{2} \lambda y) + C_{w1}^{(2)} \sinh(\sqrt{2} \lambda y) \\ & + C_{w1}^{(3)} y + C_{w1}^{(4)} \end{aligned} \quad (9)$$

where $C_{w1}^{(k)}$ ($k = 1, 2, 3, 4$) denote unknown constants. The displacement boundary conditions for $f_{w1}(y)$ at the two edges $y = 0$ and $y = b$ can be written as:

$$\begin{cases} f_{w1}(0) = w_{1i} & f_{w1}(b) = w_{1j} \\ f'_{w1}(0) = \theta_{1i} & f'_{w1}(b) = \theta_{1j} \end{cases} \quad (10)$$

where the subscript 1 is used because they are initial buckling quantities and the subscripts i and j denote amplitudes at edges i and j of the strip, respectively.

These buckling displacement amplitudes can be written as the displacement vector:

$$\tilde{d}_1 = \begin{Bmatrix} w_{1i} \\ \theta_{1i} \\ w_{1j} \\ \theta_{1j} \end{Bmatrix} \quad (11)$$

The four unknown constants $C_{w_1}^{(k)}$ ($k = 1, 2, 3, 4$) corresponding to a given strip can be fully determined in terms of buckling displacement amplitudes by substituting the boundary conditions of Eq. (10) into Eq. (7), (8) or (9). Thus, the solution of Eq. (6) can be obtained analytically in terms of the edge displacements \tilde{d}_1 . Substituting Eq. (5) into Eq. (2) yields the force boundary conditions as:

$$\begin{cases} P_{1zi} = D [f_{w_1}'''(0) - (2 - \nu)\lambda^2\theta_{1i}] \\ P_{1zj} = -D [f_{w_1}'''(b) - (2 - \nu)\lambda^2\theta_{1j}] \\ M_{1yi} = -D [f_{w_1}''(0) - \nu\lambda^2w_{1i}] \\ M_{1yj} = D [f_{w_1}''(b) - \nu\lambda^2w_{1j}] \end{cases} \quad (12)$$

The left-hand sides of Eq. (12) are the amplitudes of the buckling forces and moments at the corresponding edges of the strip. They can be written as the force vector:

$$\tilde{p}_1 = \begin{Bmatrix} P_{1zi} \\ M_{1yi} \\ P_{1zj} \\ M_{1yj} \end{Bmatrix} \quad (13)$$

The above equation which describes the edge forces in terms of the edge displacements can be re-arranged as:

$$\tilde{p}_1 = \tilde{k}_1 \tilde{d}_1 \quad (14)$$

where \tilde{k}_1 denotes the strip out-of-plane stiffness matrix. By applying these expressions to obtain the stiffness matrices of individual strips, the exact overall stiffness matrix \tilde{K}_1 for the whole structure can be assembled by using the conventional routines of the finite element analysis. The corresponding buckling problem can finally be expressed as the eigenvalue problem:

$$\tilde{K}_1(\sigma) \tilde{D}_1 = 0 \quad (15)$$

where the vector \tilde{D}_1 consists of the out-of-plane displacement amplitudes (w_1, θ_1) for each nodal line, and \tilde{K}_1 is the stiffness matrix whose coefficients include trigonometric and hyperbolic functions involving longitudinal stress σ as the strip is analyzed exactly by solving its governing differential equation.

It is realized that application of the exact method to the buckling of structures has resulted in a transcendental eigenvalue problem in the form of Eq. (15) as distinct from equation $(\tilde{K} - \sigma \tilde{K}_G) \tilde{D} = 0$ which is encountered when approximate methods such as the finite strip method are used. In this paper, two secure methods (*i.e.* bisection method and recursive Newton method) for finding the buckling load and the corresponding buckling mode of the plate structures are used [16-20].

Post-buckling analysis

After obtaining the exact shapes of buckling modes from the buckling analysis, the analysis of post-buckling behavior can proceed on the assumption that the deflected form after the buckling is a combination of the first, second and higher (if required) modes of buckling. Thus, the post-buckling out-of-plane deflection function w_2 can be written as:

$$w_2(x, y) = \sum_{q=1}^n \delta_q w_{1q}(x, y) \quad (16)$$

where δ_q are the deflection coefficients and n is the number of the required buckling modes. The in-plane boundary conditions at the loaded ends of the strip are summarized as follows:

$$N_{xy} = 0 \quad \text{at } x = 0 \ \& \ L, \quad u_2 = \begin{cases} 0 & x = 0 \\ -\varepsilon L & x = L \end{cases} \quad (17)$$

By adopting the semi-energy post-buckling procedure in the manner described in Ref. [16], the out-of-plane displacement w_2 is then substituted in the Von-Karman's compatibility equation in order to find the corresponding in-plane displacement functions as follows:

$$u_2(x, y) = -\varepsilon x + \sum_{q=1}^n \sum_{s=1}^n \delta_q \delta_s f_{qs}^{u_2}(y) \sin(2\lambda x) \quad (18)$$

$$v_2(x, y) = \nu \varepsilon y + \sum_{q=1}^n \sum_{s=1}^n \delta_q \delta_s (g_{qs}^{v_2}(y) + f_{qs}^{v_2}(y) \cos(2\lambda x) - f_{qs}^{v_2}(0)) + v_2(0, 0) \quad (19)$$

where

$$\begin{aligned} f_{qs}^{u_2}(y) &= \frac{\lambda}{4} \left(\Phi_{qs}''(y) + 4\nu\lambda^2 \Phi_{qs}(y) - \frac{1}{2} f_q f_s \right) \\ g_{qs}^{v_2}(y) &= - \int_0^y \frac{1}{4} (\varepsilon \lambda^2 f_q f_s + f_q' f_s') dy \\ f_{qs}^{v_2}(y) &= \frac{1}{8} (\Phi_{qs}'''(y) - 4(2 + \nu)\lambda^2 \Phi_{qs}'(y) + f_q f_s') \end{aligned} \quad (20)$$

and function $\Phi(y)$ can be found from the following equation:

$$\Phi_{qs}'''' - 8\lambda^2 \Phi_{qs}'' + 16\lambda^4 \Phi_{qs} = f'_q f'_s - f_q f''_s \quad (21)$$

It is noted that the first term on the right hand side of Eq. (18) represents the prescribed uniform end-shortening strain. The amplitude of the second term on the right hand side of Eq. (18), whilst evaluated at $y = 0$ and $y = b$ (*i.e.* $f_{qs}^{u2}(0)$, $f_{qs}^{v2}(b)$), represents the post-buckling in-plane displacement parameters u_{2iqs} and u_{2jq_s} , respectively (see Figure 1).

Also, the first term on the right hand side of Eq. (19) describes the transverse in-plane expansion of the strip, which occurs due to the Poisson's ratio effect. The second term describes the transverse in-plane movement of the longitudinal fibers of the strip. This movement, which is constant along the length of a given fiber, varies from a minimum value of zero at edge $y = 0$ to its maximum value at the edge $y = b$. The third term describes the in-plane waviness of the longitudinal fibers. The amplitude of this term, whilst evaluated at $y = 0$ and $y = b$ (*i.e.* $f_{qs}^{v2}(0)$; $f_{qs}^{v2}(b)$), represents the post-buckling in-plane displacement parameters v_{2iqs} and v_{2jq_s} , respectively (see Figure 1). Finally, the fourth term and the fifth term on the right hand side of Eq. (19) represent values which remain constant at all points on a given strip. It is also noted that the post-buckling in-plane displacements u_2 and v_2 are functions of out-of-plane buckling deflection modes (which are functions of critical longitudinal stresses) and deflection coefficients δ_q .

After obtaining the in-plane displacements, the in-plane shear force and in-plane transverse force can be calculated from Eq. (2) as the following set of linear equations:

$$\tilde{p}_{2qs} = \tilde{k}_{2qs} \tilde{d}_{2qs} + \tilde{f}_{2qs} \quad (22)$$

where

$$\tilde{d}_{2qs} = \left\{ u_{2iqs}, v_{2iqs}, u_{2jq_s}, v_{2jq_s} \right\}^T \quad (23)$$

and

$$\tilde{p}_{2qs} = \left\{ P_{2xiqs}, P_{2yiqs}, P_{2xjq_s}, P_{2yjq_s} \right\}^T \quad (24)$$

\tilde{f}_{2qs} consists of terms corresponding to the out-of-plane displacement parameters, and \tilde{k}_{2qs} consists of terms corresponding to the in-plane displacement parameters (*i.e.* u_{2qs} , v_{2qs}) which is the stiffness matrix of the strip. The overall stiffness equations corresponding to the whole structure are formed by following the conventional finite element assembly procedure, and noting that the structure is not subjected to any

external force; thus, \tilde{p}_{2qs} vector vanishes during the assembly process. The overall stiffness equations are:

$$\tilde{K}_{2qs} \tilde{D}_{2qs} = \tilde{F}_{2qs} \quad (25)$$

where matrices \tilde{K}_{2qs} , \tilde{D}_{2qs} and \tilde{F}_{2qs} are assembled from their counterparts (*i.e.* \tilde{k}_{2qs} , \tilde{d}_{2qs} and \tilde{f}_{2qs}) for each strip. Once Eq. (25) is solved and the post-buckling in-plane displacement parameters are obtained, they are then substituted into Eq. (18) and (19) to determine the analytical form of u_2 and v_2 for each strip, respectively. It is noted that the obtained u_2 and v_2 and the assumed w_2 are all determined in terms of the deflection coefficients δ_q , which will be calculated below.

Deflection coefficients (δ_q) calculation

For a prescribed uniform end-shortening strain ε , the total strain energy of the structure $U = \sum U_s$, which is simply equal to its total potential energy, can be expressed as follows:

$$U = m_0 \varepsilon^2 + \sum_{q=1}^n \sum_{s=1}^n \delta_q \delta_s (b_{2qs} - \varepsilon m_{2qs}) + \sum_{q=1}^n \sum_{\bar{q}=1}^n \sum_{s=1}^n \sum_{\bar{s}=1}^n \delta_q \delta_{\bar{q}} \delta_s \delta_{\bar{s}} m_{4q\bar{q}s\bar{s}} \quad (26)$$

where

$$\begin{aligned} m_{4q\bar{q}s\bar{s}} &= \sum \frac{1}{32} t E \lambda^4 L \left(\int_0^b (f_q f_{\bar{q}} f_s f_{\bar{s}} + 2\Phi_{qs}'' \Phi_{\bar{q}\bar{s}}'' \right. \\ &\quad \left. + 16\lambda^2 \nu \Phi_{qs} \Phi_{\bar{q}\bar{s}}'' + 16\lambda^2 (1 + \nu) \Phi_{qs}' \Phi_{\bar{q}\bar{s}}' \right. \\ &\quad \left. + 32\lambda^4 \Phi_{qs} \Phi_{\bar{q}\bar{s}} \right) dy \\ m_{2qs} &= \sum \frac{1}{4} t E L \lambda^2 \int_0^b f_q f_s dy \\ m_0 &= \sum \frac{1}{2} t E L b \\ b_{2qs} &= \sum \frac{1}{4} L D \int (\lambda^4 f_q f_s - 2\lambda^2 (1 - \nu) f'_q f'_s \\ &\quad - 2\lambda^2 (\nu - 2) f_q f''_s + f''_q f''_s) dy \end{aligned} \quad (27)$$

Here, the summation \sum relates to all strips. In evaluating the above constants, all integrations are determined analytically. It is emphasized that these constants need to be evaluated once. It is noted that the deflection coefficients δ_q are the only unknowns in the energy expression. The strain energy is then minimized by differentiating U with respect to each δ_q . The obtained set of nonlinear equations is solved

by using Newton-Raphson procedure. Once the global equilibrium equations are solved and the deflection coefficients are found for a particular prescribed end-shortening, it is possible to calculate all displacements, strains and stresses.

THEORETICAL DEVELOPMENTS OF THE SEMI-ANALYTICAL FSM

The theoretical development of the Semi-analytical FSM (S-a FSM) for the post-buckling analysis of the isotropic plates is presented in this section. It is emphasized that in the semi-analytical finite strip approach, all the displacements are postulated by the appropriate shape functions while in the development process of the full-analytical approach, the displacement fields were obtained by solving the Von-Karman's equations. The displacement fields of the single term S-a FSM are expressed as:

$$u = -\varepsilon x + f_u(y) \sin\left(\frac{2\pi x}{L}\right) \quad (28)$$

$$v = \nu \varepsilon y + f_v^0(y) + f_v(y) \cos\left(\frac{2\pi x}{L}\right) \quad (29)$$

$$w = f_w(y) \sin\left(\frac{\pi x}{L}\right) \quad (30)$$

The f_u, f_v^0, f_v and f_w are transverse polynomial interpolation functions of various types and orders, involving undetermined displacement coefficients. It is noted that in obtaining the S-a FSM results, in addition to the application of the linear Lagrange polynomial interpolation functions for the in-plane displacements u and v , as noted in Ref. [21], the quadratic polynomial interpolation functions are also used. In representing w , the cubic Hermitian polynomial is utilized as explained in Ref. [21].

With the establishment of the finite strip displacement fields according to the equations mentioned above, the strain energy of the strip which is equal to its total potential energy can ultimately be obtained. For the whole structure, comprising an assembly of finite strips, the total potential energy is simply the summation of the potential energies of the individual finite strips [13-15]. The pertinent structure equilibrium equations are obtained by applying the principle of minimum potential energy. That is to say, the partial differentiation of the structure potential energy with respect to each degree of freedom, in turn, gives a set of non-linear equilibrium equations which needs to be modified by applying the appropriate zero-displacement boundary conditions at the longitudinal exterior edges. After the application of any appropriate zero-displacement boundary conditions, the equations

must be solved. In the present study, the Newton-Raphson (N-R) iterative procedure is selected for solving the equations as in the previous section.

Once the global equilibrium equations are solved and the degrees of freedom are found for a particular prescribed end-shortening, it is possible to calculate all displacements, strains and stresses.

RESULTS AND DISCUSSIONS

A plate with the width to thickness ratio b/t of 100 and the Poisson's ratio ν of 0.3 is considered. The loaded edges of the plate are simply supported as described earlier whilst the out-of-plane boundary conditions at the two unloaded edges are clamped-simply supported (SCSS). The in-plane transverse displacement is allowed to occur at the unloaded edges. In the case of F-a FSM analysis, the plate is initially divided into two, four and ten strips of equal width giving three cases for consideration. The investigation of the results has revealed that the critical buckling load and the post-buckling results are identical among the three cases as expected. Thus, a plate can be accurately modelled by applying only one strip to it. However, in the case of S-a FSM analysis, in order to obtain converged results, at least 32 or 16 strips are needed when the linear or quadratic interpolation functions are used, respectively.

After the buckling analysis carried out by using F-a FSM, the first five out-of-plane buckling deflection

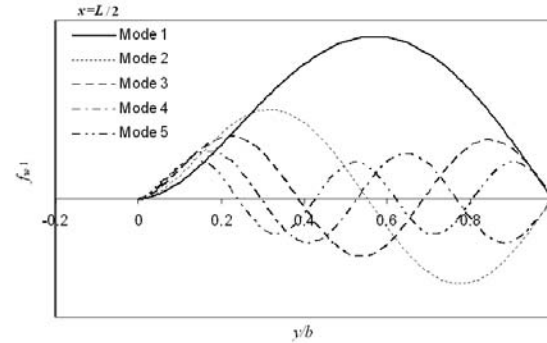


Figure 2. Out-of-plane buckling deflection modes in transverse direction for SCSS plate.

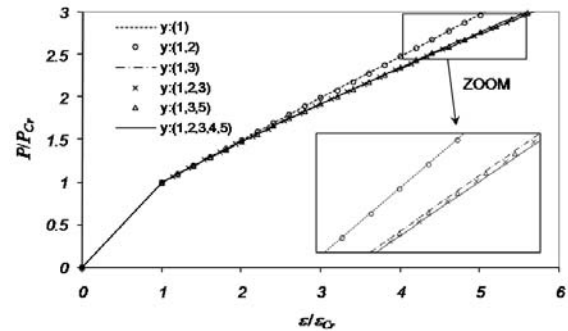


Figure 3. Convergence study of F-a FSM analysis.

modes of this plate can be obtained as follows:

$$f_{1,w1}(y) = 0.64112 \cosh(0.029y) - 0.64113 \sinh(0.029y) \\ - 0.64112 \cos(0.019y) + \sin(0.019y)$$

$$f_{2,w1}(y) = 0.84374 \cosh(0.041y) - 0.84374 \sinh(0.041y) \\ - 0.84374 \cos(0.035y) + \sin(0.035y)$$

$$f_{3,w1}(y) = 0.91632 \cosh(0.055y) - 0.91632 \sinh(0.055y) \\ - 0.91632 \cos(0.05y) + \sin(0.05y)$$

$$f_{4,w1}(y) = 0.94866 \cosh(0.07y) - 0.94866 \sinh(0.07y) \\ - 0.94866 \cos(0.0666y) + \sin(0.0666y)$$

$$f_{5,w1}(y) = 0.96551 \cosh(0.085y) - 0.96551 \sinh(0.085y) \\ - 0.96551 \cos(0.082y) + \sin(0.082y) \quad (31)$$

The variations of these modes in transverse direction are depicted in Figure 2. As can be seen, the out-of-plane buckling deflection modes of a SCSS plate include trigonometric and hyperbolic functions.

The non-dimensional load-end shortening variations ($P/P_{Cr} - \varepsilon/\varepsilon_{Cr}$) are depicted in Figure 3 where the convergence study with respect to the number of buckling modes assumed in the F-a FSM analysis is also investigated. It is noted that for the plate under consideration, the number of buckle half-wavelengths along the plate (*i.e.* parameter \bar{n} in Eq. 5) is assumed to be equal to one. Thus, the buckling modes are different in their representation in the transverse y direction. For example, the symbol $y:(1,3)$ is used to refer to the case where the first and the third modes in the y direction are considered. The nonlinear nature of the behavior, which happens due to the effects of change in the deflection coefficients δ_q , can be clearly seen for the cases where several modes are considered. It is seen that in the advanced stages of post-buckling, the combination of the first three buckling modes, *i.e.* $y:(1,2,3)$, has led to the results with high accuracy. Nevertheless, for further assurance in the remainder of the paper, the results are presented by assuming the first five buckling modes in the case of F-a FSM analysis.

In order to investigate the validation of the proposed methods, the load-end shortening variations obtained by the developed F-a FSM and S-a FSM are compared in Figure 4. Two types of S-a FSM results, which are obtained by either linear or quadratic interpolation functions, are presented. The figure shows that the results of the F-a FSM agree very well, particularly with those obtained by the quadratic S-a FSM. It is noted that, in comparison to the linear S-a FSM, the quadratic S-a FSM has delivered slightly more accurate results by implementing less strips.

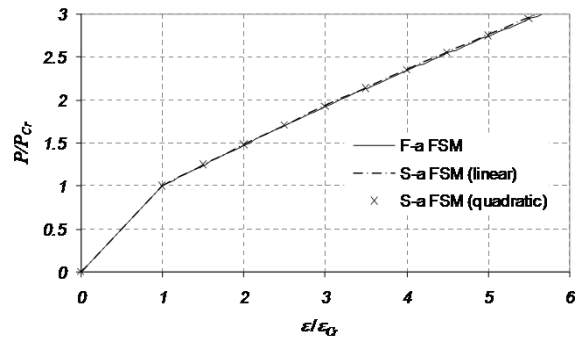


Figure 4. Variations of the non-dimensional load-end shortening.

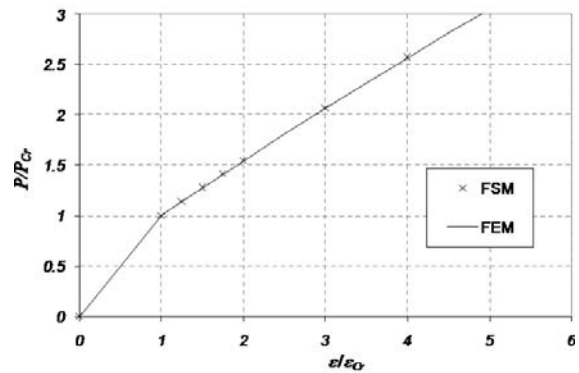


Figure 5. Comparison between the FSM and FEM results.

As can be seen, the validation of the newly developed full analytical FSM is attempted by comparing the results with those obtained by the semi-analytical FSM method. But the degree of accuracy of the semi-analytical FSM, which is used for the validation, is approved in the authors' previous publication [13] by comparing the FSM results with those obtained by FEM. For completeness and to attain a full understanding of concepts in a single paper, this comparison is repeated in Figure 5.

In order to obtain the results, a plate with a length to width ratio of 2, which was clamped out-of-plane at one unloaded edge, and was free on the other edge (*i.e.* C-F), was considered. This plate had a Poisson's ratio ν of 1/3. The unloaded edges were assumed to be unconstrained in-plane. In order to obtain the FEM results, the geometric non-linear FEM analysis was carried out for plate under consideration employing the MSC/NASTRAN finite element package. The CQUAD4 element was used to model the plate. After performing the appropriate convergence study with respect to the number of elements, a total of 288 square elements were considered to be sufficient for delivering accurate results.

As can be seen again, the semi analytical FSM results agree well with the FEM results. Thus, the semi-

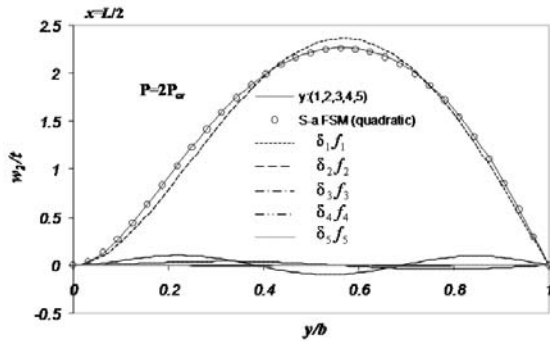


Figure 6. The out-of-plane deflected shape across the plate at the crest of the buckle.

analytical FSM is considered to be a good platform for the validation of the full-analytical FSM results.

Figure 6 represents the deflected shape at the crest of the buckle (*i.e.* at $x = L/2$) at twice the buckling load. As far as the F-a FSM results are concerned, the contribution of different buckling modes is depicted separately. In other words, the linear summation of the deflections corresponding to $\delta_1 f_1$ to $\delta_5 f_5$ has led to the total deflection of the plate, which is designated by the symbol $y:(1,2,3,4,5)$. It is seen that the total deflection of the plate is mainly governed by the contribution from the first buckling mode (*i.e.* $\delta_1 f_1$). It is also seen that the deflected shape obtained by the F-a FSM agrees very well with that of S-a FSM. However, it is worth mentioning that the results of F-a FSM are achieved by employing only one strip and 5 degrees of freedom (*i.e.* δ_1 to δ_5), whereas the quadratic S-a FSM analysis is accomplished by applying 16 strips and 130 degrees of freedom.

CONCLUSION

Theoretical developments of two finite strip methods (*i.e.* semi-analytical and full-analytical) for the post-buckling analysis of some isotropic flat plates have been presented here. In the S-a FSM post-buckling approach, all the displacements are postulated by the appropriate shape functions whilst in the development process of the F-a FSM approach, the Von-Karman's equilibrium equation is solved exactly to obtain the buckling loads and the corresponding forms of out-of-plane buckling deflection modes. The F-a FSM post-buckling study is then attempted with the assumption that the deflected form after the buckling is the combination of the first, second and higher (if required) modes of buckling, and the so-called semi-energy method is utilized. It is realised that the F-a FSM analysis is benefiting from a considerably less computational effort due to the implementation of a single strip, as compared to that of S-a FSM which requires at least 16 strips to deliver converged results for the cases considered in this paper.

REFERENCES

1. Lau S.C.W, Hancock G.J., "Buckling of Thin Flat-Walled Structures by a Spline Finite Strip Method", *Thin-Walled Struct.*, **4**, PP 269-294(1986).
2. Dawe D.J., Craig T.J., "Buckling and vibration of shear deformable prismatic plate structures by a complex finite strip method", *Int. J. of Mech. Sci.*, **30**, PP 77-79(1988).
3. Wang S., Dawe D.J., "Buckling of composite shell structures using the spline finite strip method", *Compos.: Part B*, **30**, PP 351-364(1999).
4. Zou G.P., Lam S.S.E., "Buckling analysis of composite laminates under end shortening by higher-order shear deformable finite strips", *Int. J. for Numer. Meth. in Eng.*, **55**, PP 1239-1254(2002).
5. Cheung Y.K., Kong J., "The Application of a new finite strip to the free vibration of rectangular plates of varying complexity", *J. of Sound and Vib.*, **181**, PP 341-353(1995).
6. Graves Smith T.R. and Sridharan S., "A finite strip method for the post-locally-buckled analysis of plate structures", *Int. J. of Mech. Sci.*, **20**, PP 833-842(1978).
7. Sridharan S. and Graves-Smith T.R., "Post-buckling analysis with finite strips", *J. Eng. Mech. Div., ASCE*, **107**, PP 869-88(1981).
8. Hancock G.J., "Nonlinear Analysis of Thin Sections in Compression", *J. Struct. Div. (ASCE)*, **107**, PP 455-471(1981).
9. Dawe D.J., "Use of the finite strip method in predicting the behaviour of composite laminated structures", *Compos. Struct.*, **57**, PP 11-36(2002).
10. Rhodes J., "Research into thin-walled structures at the university of Strathclyde - A brief history", *Published in the Conference Proceedings of Bicentenary Conference on Thin-Walled Structures*, (1996).
11. Chou S.M. and Rhodes J., "Review and compilation of experimental results on thin-walled structures", *Computers and Structures*, **65**(47-67), (1997).
12. Khong P.W., Rhodes J., "Linear and Non Linear Analysis on the Micro Using Finite Strip", (1988).
13. Ovesy H.R., Loughlan J. and Ghannadpour S.A.M., "Geometric non-linear analysis of thin flat plates under end shortening, using different versions of the finite strip method", *Int. J. of Mech. Sci.*, **47**, PP 1923-1948(2005).
14. Ovesy H.R., Loughlan J. and Ghannadpour S.A.M., "Geometric non-linear analysis of channel sections under end shortening, using different versions of the finite strip method", *Computers and Structures*, **84**, PP 855-872(2006).
15. Ovesy H.R., Loughlan J., Ghannadpour S.A.M. and Morada G., "Geometric non-Linear analysis of box sections under end shortening, using three different versions of the finite strip method", *Thin-Walled Structures*, **44**, PP 623-637(2006).

16. Ovesy H.R. and Ghannadpour S.A.M., "An exact finite strip for the calculation of relative post-buckling stiffness of isotropic plates", *Structural Engineering and Mechanics*, **31**(2), PP 181-210(2009).
17. Ghannadpour S.A.M. and Ovesy H.R., "The application of an exact finite strip to the buckling of symmetrically laminated composite rectangular plates and prismatic plate structures", *Compos. Struct.*, **89**(1), PP 151-158(2009).
18. Ghannadpour S.A.M. and Ovesy H.R., "An exact finite strip for the calculation of relative post-buckling stiffness of I-section struts", *Int. J. of Mech. Sci.*, **50**(9), PP 1354-1364(2008).
19. Ghannadpour S.A.M. and Ovesy H.R., "Exact post-buckling stiffness calculation of box section struts", *Engineering Computations: Int. J. for Computer-Aided Eng. and Soft.*, **26**(7), PP 868-893(2009).
20. Ovesy H.R. and Ghannadpour S.A.M., "An Exact Finite Strip for the Initial Post-Buckling Analysis of Channel Section Struts", *Comp. Struct.*, **89**(19-20), PP 1785-1796(2011).
21. Ovesy H.R. and Ghannadpour S.A.M., "Geometric nonlinear analysis of imperfect composite laminated plates, under end shortening and pressure loading, using finite strip method", *Composite Structures*, **75**, PP 100-105(2006).